Dynamics of phosphatidylcholine-cholesterol mixed model membranes in the liquid crystalline state

Y.-K. Shin, J. K. Moscicki, and J. H. Freed
Baker Laboratory of Chemistry, Cornell University, Ithaca, New York 14853

ABSTRACT The effects of cholesterol on the dynamics of cholestane spin probe (CSL) in various phosphatidylcholine-cholesterol mixed model membranes are examined. The lateral diffusion, D of CSL in DMPC/POPC/cholesterol ternary mixtures, is measured utilizing an improved dynamic imaging electron spin resonance method. It shows a factor of two decrease at 10 mol % and 25°C, whereas it shows only a 40% decrease at 50 mol % and 50°C. A comparison with results in POPC/cholesterol mixtures, which show a stronger effect of cholesterol on D, indicates that acyl chain unsaturation leads to stronger self association of cholesterol in PC model membranes. An S^2_{CSL} dependence of the activation energy for D, has been confirmed for the DMPC/POPC/cholesterol mixtures. Here S_{CSL} is the order parameter for CSL. A similar correlation of $R_\perp$, the perpendicular component of the rotational diffusion coefficient, with S_{CSL}, which is true for all three mixtures (DMPC/cholesterol, POPC/cholesterol, and DMPC/POPC/cholesterol) we have studied, is also found. These are associated with the effects of enhanced local ordering on the free volume needed for translation and reorientation. Such correlations of dynamic properties D and $R_\perp$ with the thermodynamic quantity S, as well as the consistent interpretations of the effect of acyl chain unsaturation on the dynamics in terms of the activity coefficients, strongly emphasize the interrelation between the dynamic structure and the thermodynamics of the PC/cholesterol mixtures.

INTRODUCTION

The dynamics of binary mixtures of phosphatidylcholines (PC) and cholesterol has been studied extensively. The results have been quite diverse depending upon the type of PC used (e.g., saturated acyl chain PC and/or unsaturated acyl chain PC) as well as the type of molecular probe used (phospholipid type or sterol type).

The dynamics of phospholipid-type molecular probes, which are believed to report on the phospholipid molecules, have been studied in saturated PC (e.g., DMPC or DPPC) and cholesterol mixtures. It was observed that the lateral diffusion coefficient (D) of a fluorescence probe (NBD-PE) does not change until the cholesterol concentration reaches ~10 mol %, whereas above 10 mol %, D starts to decrease to an asymptotic value of about a factor of three less than in pure saturated PC model membranes (Rubenstein et al., 1979). The rotational mobility of PC type probes and stearic acid spin probes was found to decrease with increase of cholesterol (Recktenwald and McConnell, 1981; Kusumi et al., 1986).

To study cholesterol in binary mixtures, cholestane spin probe (CSL) has been widely used. It is observed that as the cholesterol concentration is increased, there is a decrease in rotational mobility of CSL and an increase in its ordering in saturated PC and cholesterol mixtures in the liquid crystalline state (Presti and Chan, 1982; Kar et al., 1985; Kusumi et al., 1986). The lateral diffusion of sterol type molecular probes is not well known. The result obtained by the "fluorescence recovery after photobleaching" method (FRAP) is that a sterol type fluorescence probe, which is structurally somewhat dissimilar to cholesterol because of a bulky fluorescent functional group, behaves identically to NBD-PE in the mixtures (Alecio et al., 1982).

Summarizing these results, the translational diffusion and the rotational mobility of both solvent and solute in saturated PC and cholesterol binary solution decrease with an increase of cholesterol. Also, both solute and solvent molecules become more ordered.

The existence of unsaturation in acyl chains of PC molecules, however, introduces a large discrepancy in the cholesterol effect. It was shown that the PC lateral diffusion in unsaturated PC model membranes (POPC and DOPC) was not affected by the presence of cholesterol over an extended concentration range (Lindblom et al., 1981). This was confirmed by the results on NBD-PE diffusion in DOPC and cholesterol mixtures (Kusumi et al., 1986) and by the results of 16-PC spin probe diffusion in POPC and cholesterol mixtures (Shin and Freed, 1989*a*). The rotational motion and ordering of PC type probes also shows only a slight effect from cholesterol (Merkle et al., 1987; Shin and Freed, 1989).

Whereas the dynamics of the PC type probes are almost independent of cholesterol in unsaturated PC membranes, CSL undergoes a significant change in its

0006-3495/90/03/445/15 $2.00

dynamics by the addition of cholesterol. The lateral diffusion of the cholesterol analogue spin probe CSL has been extensively studied in POPC/cholesterol mixtures in the liquid crystalline state (Shin and Freed, 1989*a*). The lateral diffusion coefficient of CSL decreases by a factor of four even at 10 mol % of cholesterol compared with the value at 0 mol %. Also the rotational diffusion coefficient is about one order of magnitude less at 30 mol %. The ordering of CSL increases abruptly and a tendency toward saturation of the ordering was observed around 10 mol %.

It appears that these results may be summarized by the statement that the dynamics of cholesterol is greatly influenced by varying the concentration of cholesterol, whereas the dynamics of unsaturated PC molecules is hardly affected in the unsaturated PC/cholesterol mixtures.

Although much information has been accumulated so far concerning the effect of cholesterol on the dynamic properties of PC model membranes, the interpretation lacked unifying principles. One deficiency has in our estimation been a lack of comparison between the dynamics and the thermodynamic properties of the mixtures (e.g., activity coefficients). The activities in the model membrane mixtures are not easily obtainable with existing experimental techniques. We have developed a simple way of estimating the activity coefficient of each component by considering the thermodynamic nature of the orientational order parameter S of each component (Shin and Freed, 1989*a*).

In our previous paper (Shin and Freed, 1989*a*), we attempted to explain the dramatic differences in the dynamics of solute and solvent in POPC/cholesterol mixtures in terms of thermodynamic properties. We found simple correlations of D and $R_\perp$ with S. We also found universal behavior for S vs. a scaled temperature for both CSL and 16-PC spin probes, which showed that the *disorder* parameter, $(1 - S)$ can be considered equivalent to a scaled temperature. Such correlations and the universality in S were interpreted as a consequence of simple nonideal solution behavior. Furthermore, it was shown that the profound effect of cholesterol on D_{CSL} and R_{CSL} and the very small effect of cholesterol on D_{16-PC} and R_{16-PC} were consistent with the behavior of the activity coefficients γ. (That is, γ_{chol} decreases by a factor of five when the cholesterol mole fraction x is increased from 0 to 0.3, whereas γ_{PC} increases only 13% upon x increasing from 0 to 0.2.) This not only verifies the simple nonideal solution nature of POPC/cholesterol mixtures, but also emphasizes consistency in the dynamic structure and the thermodynamics.

We intend in the present work to extend our study to various PC/cholesterol mixtures to verify if our model of the dynamic structure is consistent with the overall thermodynamic picture (Shin & Freed, 1989*b*). We also wish to determine whether general correlations of the dynamic properties D and R with the thermodynamic property S, would be applicable to all PC/cholesterol mixtures. We have already reported on the effect of acyl chain unsaturation on S (Shin and Freed, 1989*b*), and in the present study we also wish to clarify the effects on the dynamics caused by acyl chain unsaturation.

There have been a few studies concerning cholesterol affinity to a certain type of phosphatidylcholine in multicomponent PC mixtures (Verkleij elt al., 1974; De Kruyff et al., 1974). It was shown that cholesterol interacts preferentially with unsaturated PC in unsaturated PC/saturated PC mixtures when the saturated PC passed from liquid crystalline state to gel state upon lowering the temperature (Verkleij et al., 1974). On the other hand, it has been shown that acyl chain unsaturation leads to stronger self association of cholesterol in the liquid crystalline state above 35°C (Shin and Freed, 1989*b*)

We utilized an improved method of analysis in determining the lateral diffusion coefficient by the electron spin resonance (ESR) imaging technique (Moscicki et al., 1989 and 1990). The influence of experimental noise present in the analysis in Fourier transform (or k-space) is better understood as a result. Consequently the accuracy and the reliability of the diffusion measurement is significantly improved.

EXPERIMENTAL METHODS

Materials

1-Palmitoyl-2-oleoyl-*sn*-glycero-phosphatidylcholine (POPC) and 1,2-dimyristoyl-*sn*-glycero-phosphatidylcholine (DMPC) were purchased from Avanti Polar Lipids Inc. (Birmingham, AL) and were used without further purification. Cholesterol was obtained from Sigma Chemical Co. (St. Louis, MO) and recrystallized in ethanol. The 3-doxyl derivative of cholestan-3-one (CSL) was purchased from Syvar Co. (Palo Alto, CA).

Sample preparation

The two basic requirements for a good sample in our ESR imaging experiment are: (*a*) the spin probe distribution is localized at the middle of the sample; (*b*) the sample is a well-aligned homeotropic monodomain of lipid multilayers. The minimum experimental time required to successfully measure the diffusion coefficient D is determined by the equation (Moscicki et al., 1989*a* and *b*)

$$t \sim \frac{\delta^2 + (\Delta/B')^2}{D} \frac{1 + \ln \epsilon}{\epsilon \ln \epsilon - 2}, \quad (1)$$

where δ is the initial width of the concentration profile, Δ is the linewidth of the ESR spectrum, B' is the linear magnetic field gradient, and ϵ the signal-to-noise ratio in Fourier transform, or k-space (cf. Data Analysis). Thus, one has to prepare a sample of narrow initial spin probe

distribution. To prepare samples satisfying such requirements, we followed the modified evaporation-compression technique explained in our previous work (Cleary et al., 1988). It is based on the hydration-evaporation technique (Jost and Griffith, 1973) and the compression alignment technique of Tanaka and Freed (1984). For details of the procedures and characterization methods see Tanaka and Freed (1984) and Cleary et al. (1988). The spin probe concentration of the CSL was 0.75 mol % at which the ESR spectrum does not show any lineshape broadening due to Heisenberg spin exchange. The water content of the sample was determined by weighing after the ESR measurement. The DMPC/POPC/cholesterol land DMPC/cholesterol samples were found to have ~17% water by weight.

Instrumental aspects and data collection

A model E-12 spectrometer (Varian Associates, Inc., Palo Alto, Ca) was used for the experiments. The spectra were taken in the first derivative mode with 100 kHz field modulation, with a microwave power of ~8 mW, and with a modulation amplitude ~1 G. A pair of figure-eight gradient coils purchased from George Associates (Berkeley, CA), which produced a linear field gradient of 50 G/cm at 6.0 A current, were used (Moscicki et al., 1989). A standard nitrogen flowing temperature control unit (Bruker Instruments, Inc., Billerica, MA) was used to regulate the sample temperature. Temperature control and variation was achieved by using an 11-mm OD single-wall quartz dewar and by monitoring the temperature with a thermocouple inserted inside the dewar from the bottom. The temperature was controlled to ±0.5°C accuracy. The temperature of the sample was raised ~10°C between successive temperature runs. Data were collected on a Leading Edge Inc. (Canton, MA) model D PC interfaced to an HP3457 multimeter (Hewlett-Packard Co., Loveland, CO). All spectra were digitized to 1,024 points, had 100-G sweep widths, and 60-s sweep times. A gradient-off spectrum was taken after ~20 gradient-on spectra were recorded at a fixed temperature. The experimental time was ~2 h. Each sample was used for four different temperatures ranging from 25° to 55°C.

Data analysis

Dynamic imaging of diffusion by electron spin resonance

When one prepares a sample with an inhomogeneous distribution of spin probes along a given direction, the distribution tends toward homogeneity by translational diffusion. The time variation of the concentration $C(x,t)$ is expressed by the diffusion equation,

$$\frac{\partial C(x,t)}{\partial t} = D\frac{\partial^2 C(x,t)}{\partial x^2}, \tag{2}$$

where D is the diffusion coefficient. If one knows the distribution for at least two different times, one is able to calculate the diffusion coefficient from Eq. 2 (Hornak et al., 1986). The ESR imaging method provides a way of measuring the concentration profile along a given direction by the aid of a magnetic field gradient. It has been demonstrated that the method is greatly improved by studying the change of concentration profile with time in the spatial Fourier transform or k-space. The one dimensional diffusion equation in k-space is given by (Cleary et al., 1988; Moscicki et al., 1989*a*):

$$\ln|C(k,t_i)| - \ln|C(k,t_j)| = -4\pi^2 Dk^2\Delta t_{ij}, \tag{3}$$

where Δ_{ij} is the time difference between two measurements. The concentration profile is obtained in k-space utilizing the Fourier convolution theorem:

$$C(k,t_i) = \frac{I_g(k,t_i)}{I_0(k)}, \tag{4}$$

where $I_g(k,t_i)$ is the Fourier transformed gradient-on spectrum at time t_i and $I_0(k)$ is a Fourier transformed gradient-off spectrum.

Samples that are well approximated as having a gaussian concentration profile were used in our previous work (Cleary et al., 1988; Shin and Freed, 1989*a*). In such cases, the diffusion coefficient was obtained in two steps: (*a*) the width of the gaussian profile was calculated by plotting $\ln C(k,t_i)$ vs. k^2; (*b*) the width was plotted vs. time t_i. In reality, it is not so easy to prepare a sample which has a gaussian spin probe distribution. For samples which have an arbitrary concentration profile, the analysis can be performed by "pairing" the profiles at different instances of time (Cleary et al., 1988).

A weakness, up to now, in the analysis of experimental data in k-space is the difficulty in locating the range of k modes that provides accurate data on the diffusion coefficient. For example, we have shown by computer simulation that the difference expressed by the left-hand side of Eq. 3 for two gaussians with different width was completely corrupted by computational round-off error at high k, demonstrating the existence of an upper bound in the useful k modes (Moscicki et al., 1989). More relevant, the experimental noise present in the ESR spectrum is a crucial factor limiting the range of useful k modes.

Given two concentration profiles obtained at different times, Eq. 3 and Eq. 4 yield:

$$\ln\frac{|I_g(k,t_i)|}{|I_g(k,t_j)|} = -4\pi^2 Dk^2\Delta t_{ij}, \tag{5}$$

where $I_0(k)$ factors out. Consequently, the gradient-off spectrum is not necessary in obtaining D (whereas it is still necessary for obtaining rotational diffusion coefficients and order parameters by the usual ESR spectral simulations). The elimination of the division by the gradient-off spectrum, with its finite noise, enhances the accuracy of the resulting D.

The experimental noise is a crucial constraint limiting the range of useful k modes. Eq. 5 tells us that the higher k modes are more significantly affected by the diffusion due to the k^2 dependence. Suppose the change of the gradient-on ESR spectrum during the time interval Δt_{ij} is small, then the left-hand side of Eq. 5 can be expanded in a Taylor series:

$$\ln\frac{|I_g(k,t_j)|}{|I_g(k,t_i)|} \sim \frac{\Delta I(k,\Delta t_{ij})}{|I_g(k,t_i)|}, \tag{6}$$

where $\Delta I(k,\Delta t_{ij})$ is the difference of the amplitudes of the two spectra at times t_i and t_j. One notes from Eq. 6 that ΔI should be at least of the order of the experimental noise for a given k mode to be useful:

$$\frac{\Delta I(k,\Delta t_{ij})}{I_g(k,t_i)} \geq \sigma, \tag{7}$$

where $\sigma = \epsilon^{-1}$ is the k-dependent inverse of the signal-to-noise ratio ($\sigma = 1/[S_n/N]$). (We define the signal in Fourier-transformed k-space as $S_n = \int I_g(\xi)\,d\xi$, where ξ is the real space variable [in units of gauss]. We note that S_n is time independent, representing a constant number of spins in the sample. The noise N is defined as: $N = |\int N(\xi)\exp(-2\pi ik\xi)\,d\xi|$, where $N(\xi)$ is the real space random noise. Because we assume the instrumental noise to be just white noise, N is constant for all k modes.) Therefore, the lower limit of useful k modes (call it k_{LB}) is

determined at the point where the difference in the magnitude in the two paired spectra starts to overcome the experimental noise.

As we pointed out above, the amplitude of the Fourier-transformed ESR spectrum does decrease with increase of k. Obviously the amplitude will be lower than the noise level at sufficiently high k. The upper bound of useful k modes may be set at the point where the amplitude is approximately equal to that of the noise.

$$\frac{|I_g(k_{UB}, t)|}{|I_g(0, t)|} \sim \sigma. \tag{8}$$

The applied magnetic field gradient is an external source of inhomogeneous broadening of the ESR spectrum. The stronger the magnetic field gradient for a given concentration profile, the lower will be k_{UB}, and vice versa. A basic requirement for a successful measurement of diffusion is, of course, $k_{LB} \leq k_{UB}$.

So far, we have described qualitatively the influence of experimental noise on the analysis in k-space. The rigorous quantitative description and the estimations of optimum experimental conditions are presented elsewhere (Moscicki et al., 1989 and 1990).

The error for each k mode can be monitored by analyzing the data in two steps. First, the diffusion coefficient for each pair is calculated by plotting $\ln |I_g(k, t_i)/I_g(k, t_j)|$ (cf. Eq. 5) with respect to $k^2\Delta t_{ij}$ for arbitrarily fixed k_{max}, (i.e., the k modes less than k_{max} are taken into account). Second, the first step is repeated for a range of values for k_{max}, and $D(k_{max})$ is obtained by averaging the values from all time pairs for each k_{max}. Fig. 1 shows how $D(k_{max})$ goes through a plateau over a limited range of k modes (for which $k_{LB} \leq k \leq k_{UB}$). It also shows that the plateau region corresponds to the minimum rms deviation in the calculated diffusion coefficients at a given k_{max}. Therefore, one can objectively choose the D at the plateau region as a reliable diffusion coefficient.

The results of D_{CSL} for DMPC/POPC/cholesterol listed in Table 1 have been obtained by the "pairing technique" described so far. At the same time we have analyzed the data by the method which may be favorable for a gaussian concentration profile (Shin and Freed, 1989*a*) for the samples in which the concentration profile is still well approximated by a Gaussian. This analysis gives the same D values as those from the "pairing technique" within experimental errors.

We note that even though the diffusion coefficient is measured from the time evolution of the concentration profile, it is a tracer diffusion coefficient (self diffusion of tracer molecule) rather than a mutual diffusion coefficient, because the concentration of spin probes is kept so low that the spatial chemical potential gradient is negligible. We shall assume that the spin-labeled sterol (CSL) properly displays the diffusive properties of cholesterol (Shin and Freed, 1989*a*).

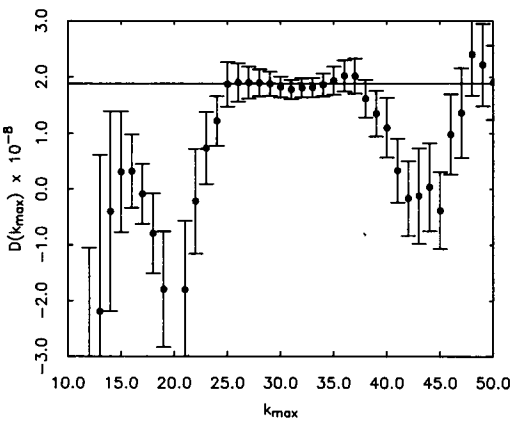

FIGURE 1 Plot of $D(k_{max})$ vs. $k_{max}(cm^{-1})$ for DMPC/POPC/cholesterol mixture with $x_{chol} = 0.215$ at 34.4°C. Error bars correspond to the standard deviation of the average of D values obtained from nine pairs. Experimental time is ~2 h. D is $1.88 \pm 0.26 \times 10^{-8}$ cm^2s^{-1}. The useful range of k modes is from 25 to 37.

Nonlinear least square spectral simulation

During the course of each experiment we collected the gradient-off spectra. They were analyzed to obtain the ordering and rotational dynamics utilizing ESR spectral simulation methods (Freed, 1976; Meirovitch et al., 1982; Schneider and Freed, 1989). The ESR simulations were performed utilizing nonlinear least square fitting to obtain the optimum parameters (Crepeau et al., 1987; Shin and Freed, 1989*a*). For CSL spin probe, we followed the axis system conventions described elsewhere (Tanaka and Freed, 1984; Meirovitch and Freed, 1984).

The potential $U(\Omega)$ determining the orientational distribution of the spin probe molecules around the ordering axis in the uniaxially ordered lipid multilayers can be expanded in a series of Wigner rotation matrix elements $D^L_{KM}(\Omega)$, e.g.,

$$-U(\Omega)/\mathcal{R}T = \lambda D^2_{00}(\Omega) + \rho[D^2_{02}(\Omega) + D^2_{0-2}(\Omega)] + \cdots \tag{9}$$

where $\mathcal{R}$ is the universal gas constant and Ω represents the Euler angles specifying the relative orientation between the principal rotational diffusion axis (it is assumed to coincide with the molecular long axis) and the ordering axis. The values of the magnetic tensor A used were $A_{x'} = 33.8$ G, $A_{x'} = 5.6$ G, and $A_{y'} = 5.3$ G for CSL. Those of g were $g_{x'} = 2.0081$, $g_{y'} = 2.0061$, and $g_{z'} = 2.0024$ (Korstanje et al., 1989). One can specify the angle (Ψ) between the ordering axis and the applied magnetic field (H_0). All spectra of CSL that were simulated had $\Psi = 0^0$, which was chosen to minimize the spectral linewidths, thereby enhancing resolution in the imaging experiments.

The first step in the nonlinear least square simulation was to choose reasonable starting values of the four parameters, λ, ρ, the perpendicular rotational diffusion coefficient ($R_\perp$), and the rotational diffusion anisotropy $N = (R_\perp/R_\parallel)$. With the $\Omega = 0$ configuration the spectral shape is sensitive mainly to perpendicular rotational diffusion coefficient and rather insensitive to rotational diffusion anisotropy N as pointed out in our previous work (Shin and Freed, 1989*a*). Thus, in the simulation we fixed $N(=R_\parallel/R_\perp)$ to 20 for 0 and 5 mol % cholesterol, 50 for 10 mol %, and 100 for >10 mol %. These are average values of N giving the minimum χ^2 for all temperatures at a given composition.

The fitting process was iterated by a Marquard-Levenberg algorithm until a minimum in the least squares was achieved. To insure that the global minimum was obtained, and to guard against spurious local minima, we restarted the algorithm several times with a range of different seed values. The orientational order parameter of CSL S_{CSL} may be obtained by integrating (Shin and Freed, 1989*a*)

$$S = \langle D^2_{00}(\Omega)\rangle = \int D^2_{00}(\Omega) \exp\left(-\frac{U(\Omega)}{\mathcal{R}T}\right) d\Omega \Big/ \int \exp\left(-\frac{U(\Omega)}{\mathcal{R}T}\right) d\Omega, \tag{10}$$

where $D^2_{00}(\Omega) = \frac{1}{2}(3\cos^2\theta - 1)$.

RESULTS AND ANALYSIS

We obtained the lateral diffusion coefficient D_{CSL}, order parameter S_{CSL}, and rotational diffusion coefficient $R_\perp$ of CSL spin probe in DMPC/POPC/cholesterol ternary mixtures for six different compositions of cholesterol, 0, 5.2, 9.9, 21.5, 35.4, and 50 mol %, cf. Table 1. The equimolar mixture of DMPC and POPC was used as the solvent. We also obtained S_{CSL} and $R_\perp$ in DMPC/cholesterol binary mixtures for the same compositions as the ternary mixtures (except for 50 mol %), cf. Table 2.

TABLE 1 Data for CSL spin probe in DMPC/POPC/cholesterol

T	D	S	λ	ρ	$R_\perp$	N
°C	$10^{-8}cm^2s^{-1}$				10^7s^{-1}	
	0 mol % cholesterol (x = 0.0)					
24.0	2.98 ± 0.16	0.685	3.78	0.67	0.63	20
34.4	3.77 ± 0.26	0.643	3.35	0.51	1.07	
45.0	5.65 ± 0.27	0.612	3.09	0.46	1.37	
55.1	7.33 ± 0.31	0.586	2.91	0.48	1.53	
	5.2 mol % cholesterol (x = 0.052)					
24.0	2.37 ± 0.20	0.758	4.66	0.75	0.52	20
34.4	3.88 ± 0.16	0.705	3.92	0.54	0.81	
45.0	5.43 ± 0.28	0.669	3.54	0.40	1.00	
55.1	7.30 ± 0.33	0.651	3.36	0.35	1.10	
	9.9 mol % cholesterol (x = 0.099)					
24.0	1.44 ± 0.12	0.831	6.41	1.40	0.23	50
34.4	2.89 ± 0.35	0.791	5.29	1.21	0.40	
45.0	4.32 ± 0.18	0.754	4.60	1.04	0.57	
55.6	6.12 ± 0.78	0.727	4.20	0.88	0.71	
	21.5 mol % cholesterol (x = 0.215)					
24.0	1.23 ± 0.26	0.861	8.24	2.68	0.14	100
34.4	1.88 ± 0.26	0.844	7.21	1.92	0.22	
45.0	3.20 ± 0.41	0.820	6.34	1.62	0.28	
55.3	5.76 ± 0.55	0.806	5.80	1.12	0.40	
	35.4 mol % cholesterol (x = 0.354)					
24.0	1.13 ± 0.25	0.896	10.9	3.78	0.10	100
26.8	1.01 ± 0.23	0.904	11.0	1.62	0.10	
28.0	1.05 ± 0.10	0.901	10.6	1.63	0.12	
31.4	1.01 ± 0.17	0.902	10.7	1.44	0.10	
33.4	1.40 ± 0.11	0.892	9.89	1.66	0.13	
34.4	1.53 ± 0.15	0.898	10.5	1.91	0.13	
36.3	1.53 ± 0.20	0.895	10.0	1.13	0.13	
40.6	1.66 ± 0.14	0.885	9.28	1.60	0.15	
45.0	3.07 ± 0.24	0.879	8.91	1.77	0.17	
50.0	4.05 ± 0.24	0.875	8.55	1.34	0.17	
55.3	6.31 ± 0.40	0.865	7.72	0.99	0.25	
	50.6 mol % cholesterol (x = 0.506)					
24.0	1.10 ± 0.10	0.915	12.2	1.02	0.09	100
34.5	1.27 ± 0.11	0.905	11.0	1.50	0.10	
45.0	2.39 ± 0.19	0.905	10.9	0.31	0.12	
55.3	4.62 ± 0.53	0.893	9.80	0.77	0.13	

The results of our previous study in POPC/cholesterol mixtures were also utilized for the analysis.

Lateral diffusion in the DMPC/POPC/cholesterol ternary mixtures

The variation of D_{CSL} vs. mole fraction of cholesterol, x at the different temperatures is shown in Fig. 2. It is noticed that in general D_{CSL} decreases in the presence of cholesterol as is the case for POPC/cholesterol mixtures (Shin and Freed, 1989*a*). D_{CSL} decreases by factors of two at 9.9 mol % and 24°C, but it decreases by only 40% at even 50 mol% and 55°C, showing a gradual weakening of the cholesterol effect on D_{CSL} upon warming. We observe that the decrease of D_{CSL} is far more prominent below 10 mol % and the further addition of cholesterol is less effective in reducing D_{CSL}.

The temperature dependence of D_{CSL} at different compositions is shown in Fig. 3. An interesting feature is that the plots of ln D_{CSL} vs. T^{-1} deviate from linearity for all compositions of cholesterol. The average activation energy of lateral diffusion at 0 mol % is 5.2 Kcal/mol. The curvature of ln D_{CSL} (x = 0.05, T) vs. T^{-1} is convex upward. At 9.9 mol % the deviation from Arrhenius behavior is even greater. Surprisingly, the nature of the deviation at low concentrations of cholesterol (5 and 10 mol %) is reversed when it is more than 20 mol %: e.g.,

TABLE 2 Data for CSL spin probe in DMPC/cholesterol

T	S	λ	ρ	$R_\perp$	N
°C				10^6s^{-1}	
	0 mol % cholesterol (x = 0.0)				
34.4	0.675	3.67	0.60	8.87	20
45.0	0.640	3.35	0.60	17.6	
55.1	0.615	3.13	0.51	24.4	
	5.2 mol % cholesterol (x = 0.052)				
34.4	0.749	4.78	1.29	3.91	20
45.0	0.692	3.96	1.00	8.09	
55.1	0.658	3.55	0.77	12.7	
	9.9 mol % cholesterol (x = 0.099)				
34.4	0.869	8.27	1.52	1.32	50
45.0	0.813	6.11	1.55	2.73	
55.6	0.764	5.01	1.29	4.49	
	21.5 mol % cholesterol (x = 0.215)				
34.4	0.917	12.4	1.72	0.89	100
45.0	0.882	8.87	1.74	1.57	
55.3	0.845	6.90	1.56	2.43	
	35.4 mol % cholesterol (x = 0.354)				
34.4	0.938	16.6	1.15	0.70	100
45.0	0.914	11.9	2.84	1.00	
55.3	0.899	10.3	1.96	1.32	

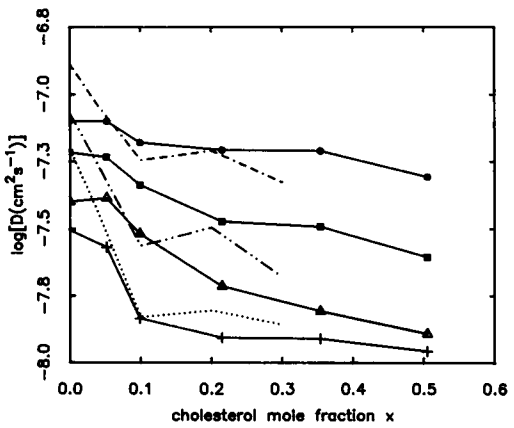

FIGURE 2 Plots of $\log D_{CSL}$ vs. x_{chol} for DMPC/POPC/cholesterol mixtures at different temperatures; 24 (+), 34.4 (△), 45.0 (■), and 55°C (●). The results are compared with D_{CSL} for POPC/cholesterol mixtures (Shin and Freed, 1989*a*); 25 (·····), 35 (— ·· — ·· —), and 48°C (—— · ——).

ln D_{CSL} ($x \geq 0.2$, T) vs. T^{-1} is convex downward. From our extensive study at 32 mol % cholesterol, it is found that two distinct types of behavior at low and at high temperature was observed for the lateral diffusion. At low temperatures ($\leq$~32°C) D_{CSL} is almost constant over the temperature range we have studied; i.e., the activation energy of lateral diffusion is close to zero. On the other hand, at temperatures higher than ~32°C, the activated diffusional process is restored with an average activation energy of ~13 Kcal/mol. It is known that a phase separation will occur at a high cholesterol concentration (Shimshick and McConnell, 1972; Kusumi et al., 1986; Shin and Freed, 1989*b*). Two such distinct types of behavior for $D_{CSL}(T)$ is likely associated with the phase separation. Our results indicate that it occurs at ~32°C and ~35 mol % of cholesterol. The same type of trend is also found for 50 mol % of cholesterol even though it was not possible to locate the exact temperature at which the phase separation occurs from our more limited data.

The results for D_{CSL} in DMPC/POPC/cholesterol mixtures are compared with those for POPC/cholesterol mixtures in Fig. 2. In the POPC and cholesterol mixtures D_{CSL} decreased by factors of four at 10 mol % of cholesterol and at 25°C, whereas it decreases by factors of two at the same concentration and temperature in the DMPC/POPC/cholesterol mixtures. At ~50°C D_{CSL} is still observed to decrease significantly in POPC/cholesterol, where it shows a factor of two decrease at 10 mol %, whereas it shows only a 40% decrease at 50 mol % in the ternary mixtures compared with those in the binary DMPC/POPC model membranes. This implies that the diffusivity of cholesterol is more strongly affected in POPC/cholesterol mixtures than in the ternary mixtures by the addition of cholesterol.

Order parameter

A thermodynamic approach to the order parameter S, whch relates the intensive thermodynamic property S_{CSL}, with the activity of cholesterol a_{chol}, has been discussed elsewhere (Shin and Freed, 1989*a* and *b*).

In Fig. 4 the order parameter S_{CSL} at 34 mol % is plotted as a function of temperature. It shows little effect of temperature on order parameter below ~32°C indicating the saturation of ordering. It decreases with temperature when the temperature is above ~32°C, which is consistent with the behavior of the inverse of the lateral diffusion coefficient.

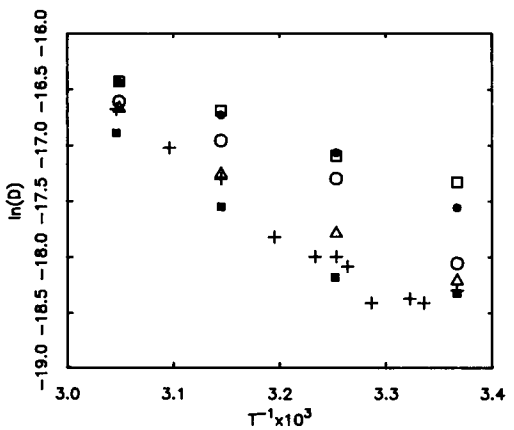

FIGURE 3 Plots of ln D_{CSL} vs. T^{-1}. Cholesterol mole fraction in DMPC/POPC/cholesterol mixtures are 0.0 (□), 0.52 (●), 0.99 (○), 0.215 (△), 0.354 (+), and 0.506 (■).

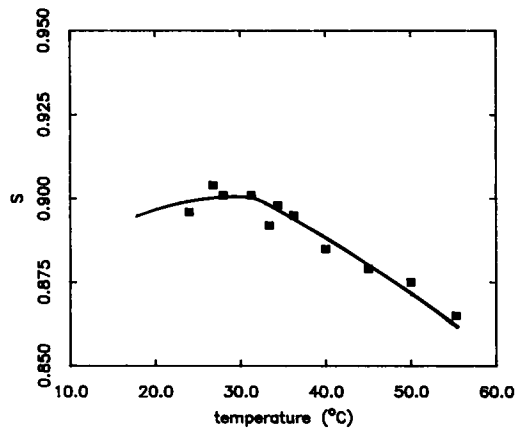

FIGURE 4 Plot of S_{CSL} vs. T at x_{chol} = 0.354 in DMPC/POPC/cholesterol mixture. The line is drawn arbitrarily to guide the eye. The two distinct types of behavior are clearly observed above and below 32°C.

Rotational diffusion

The trend of decreasing $R_\perp$ vs. cholesterol content is somewhat similar to that of the lateral diffusion coefficient as can be seen in Fig. 5 *a* and *b*, for the DMPC/cholesterol mixtures and for the DMPC/POPC/cholesterol mixtures, respectively. The effect of cholesterol is prominent at lower cholesterol concentration, except that it shows an order of magnitude decrease at 30 mol % compared with its value at 0 mol % and the effect of cholesterol is not weakened by raising the temperature.

Preference of cholesterol for various phosphatidylcholines

We have previously been able to relate the activity of cholesterol in the PC/cholesterol mixtures to $S_{CSL}(x)$ (Shin and Freed, 1989*a* and *b*):

$$S_{CSL}(x_{chol}, T) - S_{CSL}(0, T) = ba_{chol}(x_{chol}, T) = bx_{chol}\gamma_{chol}(x_{chol}, T), \quad (11)$$

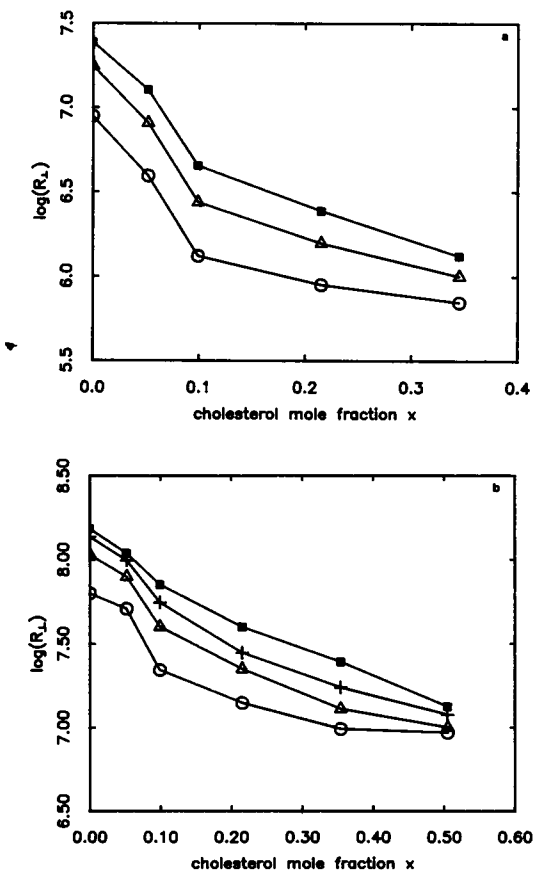

FIGURE 5 (*a*) Plots of the variation of $\log R_\perp$ of CSL with x_{chol} at different temperatures for DMPC/cholesterol mixtures: 34.4 (○), 45.0 (△), and 55°C (■). (*b*) Similar plots for DMPC/POPC/cholesterol mixtures: 24 (○), 34.4 (△), 45.0 (+), and 55°C (■).

where $a_{chol}(x_{chol}, T)$ is the activity of cholesterol at the cholesterol mole fraction, x_{chol} and $\gamma_{chol}(x_{chol}, T)$ is its associated activity coefficient.

The analysis of S_{CSL} based on Eq. 11 for the DMPC/cholesterol mixtures and the POPC/cholesterol mixtures indicated $1 > \gamma_{chol}^{DMPC} > \gamma_{chol}^{POPC}$ for all x_{chol} (Shin and Freed, 1989*b*). This suggests that cholesterol has a tendency to associate in PC/cholesterol mixtures ($\gamma_{chol} < 1$). Furthermore, the inequality ($\gamma_{chol}^{DMPC} > \gamma_{chol}^{POPC}$) implies that cholesterol tends to associate more in the POPC membrane than in the DMPC membrane. In other words, acyl chain unsaturation tends to lead to cholesterol expulsion from the vicinity of phospholipid molecules. Consequently, it leads to stronger self association of cholesterol in the POPC/cholesterol mixtures (Shin and Freed, 1989*b*).

Another approach which does not necessarily require Eq. 11, but is consistent with it is to just examine the "excess" order parameter which may be, for the ternary mixtures containing an equimolar mixture of DMPC and POPC as a solvent, defined by

$$\Delta S_{ex}(x,T) = S(x,T)_{DMPC/POPC} - \frac{S(x,T)_{DMPC} + S(x,T)_{POPC}}{2}, \quad (12)$$

where $S(x,T)_j$ is the order parameter of CSL in the solvent j. One would expect that $\Delta S_{ex}(x,T)$ vanishes if cholesterol has an equal preference for DMPC and POPC. Fig. 6 shows that $\Delta S(x,T)$ for DMPC/POPC/cholesterol mixtures is positive for all T and x. This would suggest that DMPC is the more favorable solvent for cholesterol than is POPC. [Note $S(x,T)_{DMPC} > S(x,T)_{POPC}$ for all x.] Thus, we may again conclude that cholesterol prefers DMPC in DMPC/POPC/cholesterol ternary mixtures.

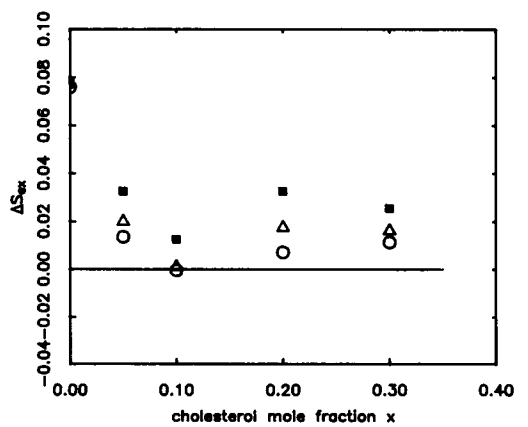

FIGURE 6 Plots of ΔS_{ex} vs. x at different temperatures: 35 (⊙), 45 (△), and 55°C (□).

Universal correlations

Correlation between D and S

In our previous work on binary model membrane solutions of POPC/cholesterol we were able to relate the lateral diffusion coefficient to the ordering (Shin and Freed, 1989*a*). It was found that the activation energy for lateral diffusion was a function of S^2, corresponding to an enhanced activation energy barrier as the ordering of the membrane is increased by addition of cholesterol. For the DMPC/POPC/cholesterol mixtures we again find that the empirical relation

$$D(S,T) = D^{\circ}(T)\exp\{-[\alpha(T)S^2/\mathcal{R}T]\} \qquad (13)$$

fits our experimental results with $\alpha(T) = -4363\mathcal{R} + 1.55 \times 10^6\mathcal{R}/T$, as is shown in Fig. 7, *a–c* (for POPC/cholesterol mixtures $\alpha(T) = -3364R + 1.3 \times 10^6\mathcal{R}/T$ [Shin and Freed, 1989*a*]). Previously $D^{\circ}(T)$ for POPC/cholesterol mixtures was found to be temperature dependent and it was expressed as $D^{\circ}(T) = D^{\circ}\exp(-\beta/\mathcal{R}T)$. But we find that $D^{\circ}(T)$ is temperature independent for the present ternary solutions within experimental scatter and it has the value $D^{\circ} = 1.16 \times 10^{-7}\ \mathrm{cm^2s^{-1}}$. Note that in Eq. 13 the only dependence of D on x is through its dependence on $S(x,T)$.

Correlation between $R_{\perp}$ and S

We suggested previously an empirical formula which showed an $(1 - S)^2$ dependence of $R_{\perp}$ for the highly ordered CSL spin probe in POPC/cholesterol mixtures. However, this relation was not found to be appropriate for DMPC/POPC/cholesterol mixtures and DMPC/cholesterol mixtures. Instead, we have found an empirical relation which is appropriate for all three PC/cholesterol mixtures that we have studied. It is

$$R_{\perp} = R_{\perp}^{\circ}\exp(-AS^2/\mathcal{R}T), \qquad (14)$$

where A is a constant for a given type of mixture. Eq. 14 implies that the activation energy of the rotational motion also depends on S^2 as is the case for translational motion. An interesting feature of Eq. 14 is that the constant A is independent of temperature, whereas in Eq. 13 α shows a rather considerable temperature dependence. $R_{\perp}^{\circ}$ is also temperature independent. The fits according to Eq. 14 are shown in Fig. 8, *a–c*, for the three mixtures. The best fitting A (in units of kilocalories per mole) and $R_{\perp}^{\circ}$ (in units of seconds^{-1}) are, respectively: 3.94 and 1.78×10^8 for DMPC/cholesterol mixtures, 2.86 and 7.26×10^7 for the POPC/cholesterol mixtures, and 3.27 and 9.79×10^7 for the ternary mixtures (errors in A and $R_{\perp}^{\circ}$ are both $<1\%$). This, of course, suggests that the activation energy barrier for the rotational motion of a CSL molecule in the DMPC/cholesterol mixtures is slightly higher than in the POPC/cholesterol mixtures.

Temperature dependence of D_{CSL} in two-phase region

The negligible temperature dependence of D_{CSL} on the right side of the phase boundary of DMPC/POPC/

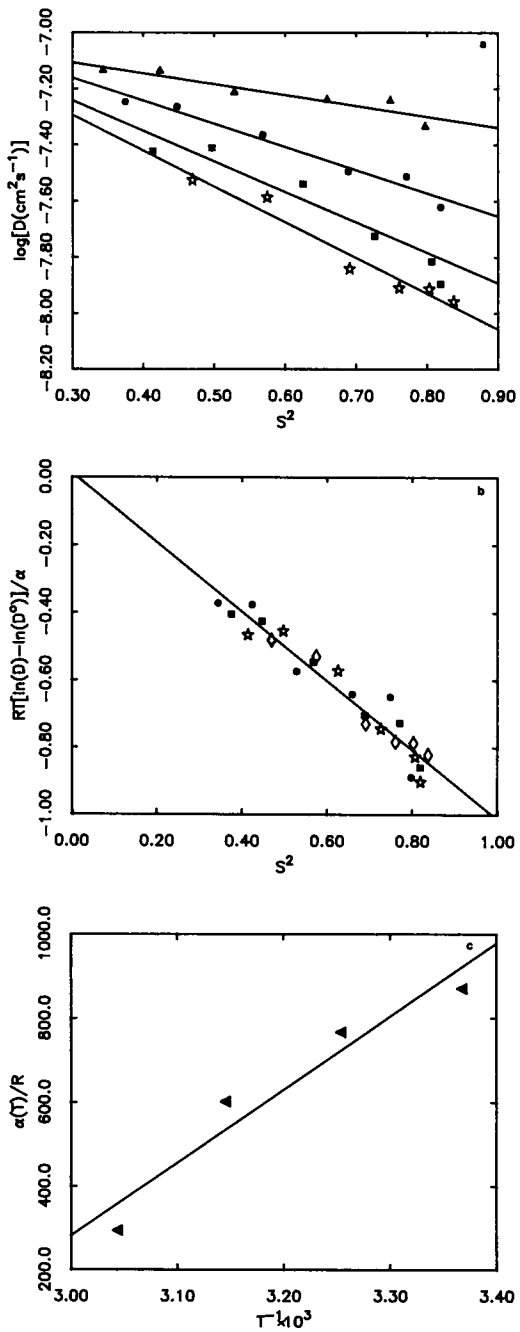

FIGURE 7 (*a*) Semilog plots of D_{CSL} vs. S^2_{CSL} at different temperatures for DMPC/POPC/cholesterol mixtures: 24 (*), 34.4 (■), 45.0 (●), and 55°C (▲). (*b*) Plot of $RT[\ln D(x,T) - \ln D^0]/\alpha$ vs. $S^2(T)$ at different temperatures: 24 (◇), 34.4 (*), 45.0 (■), and 55°C (●). (*c*) Plot of $\alpha(T)/\mathcal{R}$ vs. T^{-1} associated with *b*.

cholesterol mixtures is somewhat peculiar. Suppose this is a two-phase region as has been suggested by the thermodynamic analysis of the order parameter, and the phase separation is due to a first order phase transition. This is implied by the larger hyperfine splitting of the ESR spectrum associated with the separated phase (phase 2), which is presumably cholesterol rich and somewhat disordered (Freed and Shin, 1989*b*). Let the total number of moles in phase 1 (which should be the same phase as that to the left of the phase boundary) be N_1 which is composed of m_1 moles of lipid and n_1 moles of cholesterol. And let N_2 in phase 2 be composed of m_2 moles of lipid and n_2 moles of cholesterol. Then the mole fraction of cholesterol x_1 in phase 1 would be n_1/N_1. Likewise, x_2 in phase 2 would be n_2/N_2. The chemical potential of cholesterol in phase 1 is given by:

$$\mu_1(x,T) = \mu_1^\circ(T) + \mathcal{R}T \ln \gamma_1 x_1, \tag{15}$$

and in phase 2,

$$\mu_2(x,T) = \mu_2^\circ(T) + \mathcal{R}T \ln \gamma_2 x_2.$$

At equilibrium, μ_1 should be equal to μ_2. From this, we obtain an equilibrium condition:

$$-\frac{\mu_1^\circ - \mu_2^\circ}{\mathcal{R}T} = -\frac{\Delta\mu^\circ}{\mathcal{R}T} = \ln\frac{\gamma_1 x_1}{\gamma_2 x_2}, \tag{16}$$

or

$$n_1 = n_2 \frac{\gamma_2 N_1}{\gamma_1 N_2} \exp\left(-\frac{\Delta\mu^\circ}{\mathcal{R}T}\right).$$

Then, if we assume that as a result of the long period of measurement (~1 h), the apparent diffusion coefficient D_{CSL} measured in this region may be approximated by:

$$D_{CSL} = \frac{n_1}{n_1 + n_2} D_1 + \frac{n_2}{n_1 + n_2} D_2, \tag{17}$$

where D_i is the diffusion coefficient of cholesterol in the phase i. We have already assumed that phase 2 is composed of cholesterol-rich clusters. Then the diffusion of cholesterol in these clusters would be much slower than that in phase 1 ($D_2 \ll D_1$). Therefore, D_{CSL} is approximated by

$$D_{CSL} = \frac{n_1}{n_1 + n_2} D_1 = \frac{n_2}{n_1 + n_2} \frac{\gamma_2 N_1}{\gamma_1 N_2} \exp\left(-\frac{\Delta\mu^\circ}{\mathcal{R}T}\right) D_1. \tag{18}$$

The first order nature of the phase separation tells us that the two phases may have different Henry's law standard states ($\Delta\mu^\circ \neq 0$). If we incorporate the T and S dependence of D_1 (cf. Eq. 13) into Eq. 18, we obtain;

$$D_{CSL} = D^\circ \frac{n_2}{n_1 + n_2} \frac{\gamma_2 N_1}{\gamma_1 N_2} \exp\left(-\frac{\Delta\mu^\circ - \alpha(T)S^2}{\mathcal{R}T}\right). \tag{19}$$

Eq. 19 implies that the observed peculiar temperature dependence in the two-phase region might reflect the fact that $\Delta\mu^\circ \sim \alpha(T)S^2$, (and that the preexponential factor in Eq. 19 is weakly temperature dependent). This is

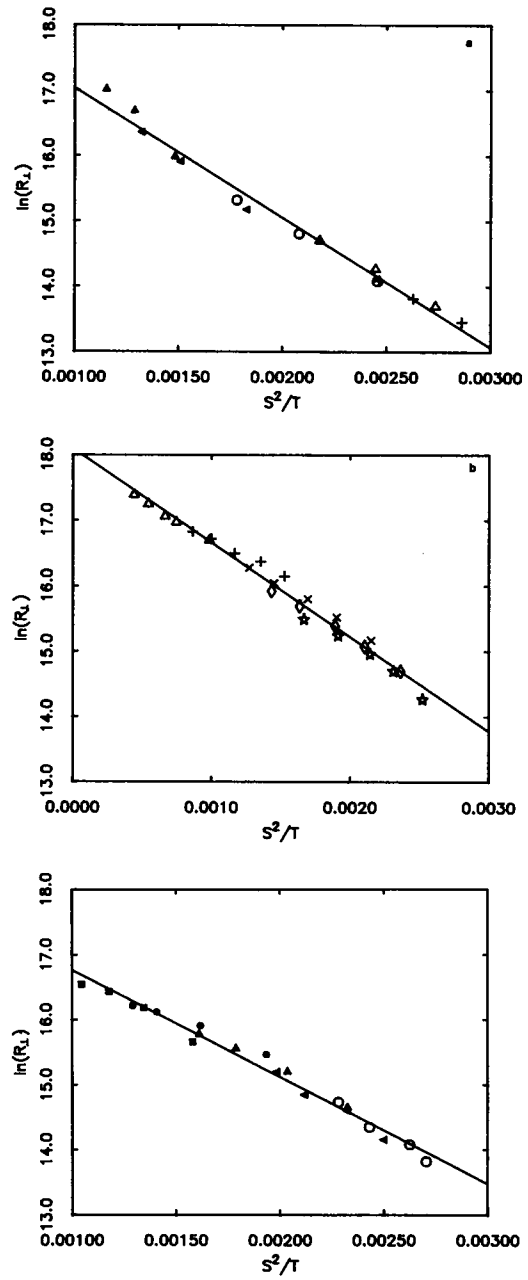

FIGURE 8 (*a*) Plots of ln $R_\perp$ vs. $S^2(T)/T$ at different x_{chol} for DMPC/cholesterol mixtures: 0.0 (▲), 0.52 (▶), 0.99 (○), 0.215 (△), and 0.354 (+). (*b*) Similar plots for POPC/cholesterol mixtures: 0.0 (△), 0.04 (+), 0.10 (x), 0.2 (◇), and 0.3 (*). (*c*) Similar plots for DMPC/POPC/cholesterol mixtures: 0.0 (■), 0.52 (●), 0.99 (▶), 0.215 (▲), and 0.354 (○).

consistent with mean field models for thermotropic liquid crystals which yield an S^2 dependence of μ° (de Gennes, 1974).

DISCUSSION

The results of the thermodynamic approach to the S_{CSL} suggested that cholesterol interacts preferentially with DMPC molecules rather than with the POPC molecules, which is consistent with the stronger self association of cholesterol in unsaturated POPC/cholesterol mixtures (Shin and Freed, 1989*b*). This suggests that cholesterol prefers DMPC to POPC (even though it tends to aggregate in either solvent) resulting in weaker association of cholesterol in DMPC/cholesterol mixtures. This could be because the interaction of cholesterol with DMPC is more favorable than with POPC, or because the unsaturated flexible POPC acyl chain does not favor rigid rodlike cholesterol molecules due to the steric hinderance. Cholesterol–cholesterol interactions are, of course, favored more than the other interactions, thereby maintaining the tendency of association of cholesterol molecules in all PC model membranes. But we conclude that cholesterol is expelled more strongly from the vicinity of an unsaturated PC than from a saturated PC.

The interpretations of the thermodynamic approach (Shin and Freed, 1989*b*) help to understand our results of lateral diffusion coefficient in ternary model membranes which show weaker dependence on cholesterol mole fraction than in POPC/cholesterol binary solutions. Because cholesterol associates less strongly, the increase of ordering in cholesterol-rich domains would not be as significant; the molecular packing in cholesterol-rich clusters would be somewhat looser, thereby letting the molecules have a better chance to diffuse. Consequently, lateral diffusion would decrease less by the addition of cholesterol in DMPC/POPC/cholesterol, compared with those in POPC/cholesterol mixtures.

Because cholesterol has a tendency to associate more in unsaturated PC model membranes, the PC molecules, which are farther from the cholesterol-rich clusters, would be less frequently encountered by cholesterol. Therefore, the dynamics of PC molecules is expected to be closer to that in pure unsaturated model membranes, in contrast to the strong effect of cholesterol on the dynamics of cholesterol analogue CSL. This is consistent with the observation that the effect of cholesterol is moderate on the lateral diffusion, the rotational diffusion, and the ESR line shape of PC analogue molecular probes from a variety of studies of unsaturated PC/cholesterol mixtures (Lindblom et al., 1981; Kusumi et al., 1986; Merkle et al., 1987).

Unlike the case of unsaturated PC/cholesterol mixtures, cholesterol is more loosely aggregated in saturated PC/cholesterol binary model membranes. Consequently, the PC molecules will more frequently encounter cholesterol, i.e., they will exhibit a higher probability to be closer to cholesterol molecules. Thus, the dynamic properties of PC molecules would be influenced more substantially by cholesterol, provided, for example, cholesterol has a tendency to immobilize nearby molecules. At the same time the dynamics of cholesterol molecules would also be appreciably affected by the association of cholesterol, even though it would be milder than in unsaturated PC model membranes.

Although it has been shown that there is a substantial effect of acyl chain unsaturation on the dynamical properties of the PC/cholesterol mixed model membranes, we find underlying universal correlations between D and S, and between $R_\perp$ and S. This shows an S^2 dependence of the activation energy of the lateral diffusion as well as of the rotational diffusion. Such correlations give an important insight into the properties of PC/cholesterol mixtures, viz. that the effect of cholesterol on the dynamical properties of the PC model membranes is mainly due to the structural change in the model membranes induced by cholesterol which is directly reflected in the change of the thermodynamic property, the order parameter. Furthermore, if we recognize that our imaging measurement of D is a macroscopic one ($\Delta x \sim 100\ \mu$m and $t \sim 1$ h), whereas those of S and R are microscopic ones (i.e., $\Delta x \sim$ molecular dimensions and $t \sim \tau_R \sim$ 10–200 ns), such correlations imply temporal and spatial uniformity characteristic of a single simple solution.

Freeze fracture experiments (Verkleij et al., 1974) and DSC studies (Van Dijck et al., 1976) showed that cholesterol prefers being in the liquid crystalline domain which would be mainly composed of the lower melting phospholipid (e.g., POPC) rather than in the gel phase domain which would be mainly composed of the higher melting phospholipid (e.g., DMPC) in ternary model membranes. Such observations are consistent with the phase diagram (Shin and Freed, 1989*b*) which shows that the phase boundaries for POPC/cholesterol mixtures and for DMPC/cholesterol mixtures cross each other at ~35°C so that the former sustains more cholesterol at lower temperatures.

We have shown that in ternary mixtures cholesterol showed less deviation from ideality than in either of the two binary mixtures (Shin and Freed, 1989*b*). This has been interpreted as the result of the entropy of mixing. For rotational motion, such a mixing effect seems not to be significant (the coefficient A in Eq. 14 for ternary mixtures is about an average of those of the two binary mixtures).

We wish to consider the S dependence of D and $R_\perp$ as expressed respectively in Eqs. 13 and 14. We have shown

that the ordering would increase either by adding cholesterol, or by lowering temperature. We can regard $\alpha(T)S^2 + \beta$ for lateral diffusion and AS^2 for rotational diffusion as the activation energy. This suggests that the activation barriers for the translational diffusion and rotational diffusion are both enhanced as membrane ordering is increased by the addition of cholesterol, or by lowering temperature (Shin and Freed, 1989*a*). The S^2 dependence of the activation energy for both translational and rotational diffusion is a prediction of a free volume model, which was originally derived by Diogo and Martins (1982) to explain the dependence of the twist viscosity on the ordering in thermotropic nematic liquid crystals. We review the relevant free volume diffusion model in the Appendix. For $R_\perp$ a linear term in S also appears in the activation energy as well as the S^2 term. This results from the (nematic) orientational potential which must be overcome to complete reorientation of the molecular long axis. However, empirically we find that the S^2 dependence is more important: the fits with an S-dependent activation energy alone are significantly poorer.

CONCLUSIONS

(*a*) The method of dynamic imaging by ESR for measuring the lateral diffusion coefficient of a spin probe in model membranes has been improved for studying spin probe concentration profiles.

(*b*) The decrease of D_{CSL} by the presence of cholesterol is consistent with the association of cholesterol in DMPC/POPC/cholesterol ternary mixtures as well as in POPC/cholesterol binary mixtures.

(*c*) The weaker effect of cholesterol on reducing D_{CSL} in DMPC/POPC/cholesterol mixtures than in POPC/cholesterol mixtures suggests a stronger expulsion of cholesterol from the vicinity of the POPC molecules than from that of the DMPC molecules. This is also consistent with the results of a thermodynamic approach to S_{CSL}, which showed that cholesterol associates more in POPC model membranes than it does in DMPC model membranes.

(*d*) We have found universal empirical relations for D_{CSL} and $R_\perp$ vs. S_{CSL}, which show an S^2_{CSL} dependence of the activation energy for both lateral diffusion and rotational diffusion, that are consistent with a free volume model and also with simple uniform solution behavior.

(*e*) The correlations, along with the thermodynamics of the phosphatidyline-cholesterol mixtures (Shin and Freed, 1989*b*), provide a comprehensive interpretation of the effect of cholesterol on model membranes in the liquid crystalline state.

(*f*) All in all, we have verified that the dynamic structure is consistent with the overall thermodynamic properties in PC/cholesterol mixtures.

APPENDIX

Free volume diffusion model: application to phospholipid/cholesterol mixed model membranes

It has been shown by Vaz et al. (1985) that plots of ln D vs. T^{-1} for a variety of saturated PC model membranes were nonlinear. They also found lateral diffusion in longer chain length PC model membranes was faster than in shorter chain length PC model membranes at the same "reduced temperature," which was the inverse of what would be expected from a hydrodynamic model. They addressed the necessity of a different theory of diffusion rather than just a hydrodynamic model. In this spirit, they utilized a free volume diffusion model to explain their results. The model proposed in their work was virtually the same as Cohen and Turnbull's (1959) original theory except that the drag forces at the membrane-water interfaces were taken into account. We also find that the viewpoint of free volume diffusion is important in the dynamics of model membrane mixtures containing cholesterol. In this appendix we consider the relevant concepts.

First of all, we briefly review the free volume diffusion model of Cohen and Turnbull. Next, we consider how to incorporate the effects of ordering in a manner applicable either to translational diffusion or to rotational diffusion. We obtain the results of Diogo and Martins (1982) slightly generalized and in a more compact fashion. Finally, we consider the case of diffusion of cholesterol in phospholipid/cholesterol model membranes.

The basic assumption of the free volume concept is that each molecule of a system is confined to a cage by its immediate neighbors. The molecule is randomly rattling inside its cage until fluctuations in density open up a hole within the cage large enough to permit a substantial displacement of the molecule. Thus, diffusion on a large scale occurs not as a result of an activation in the ordinary sense but rather as a result of redistribution of the free volume within the liquid.

Cohen and Turnbull assumed that the large scale diffusion coefficient can be written as

$$\mathcal{D} = \int_{v^*}^{\infty} \tilde{\mathcal{D}}(v)p(v)\,dv, \tag{20}$$

where $\tilde{\mathcal{D}}(v)$ (the small-scale diffusion coefficient) is an apparent contribution to the overall diffusion arising from the diffusion in a cage with the free volume of v, and $p(v)$ is the probability of occurrence of this free volume. (Note at this point that $\tilde{\mathcal{D}}(v)$ is not a diffusion coefficient in the absence of the cage, that is $\mathcal{D}^\circ$. Because the space available for diffusion is limited, the autocorrelation function of momentum [translational diffusion] or of angular momentum [rotational diffusion] decays much faster; thus, $\tilde{\mathcal{D}}(v)$ is larger than $\mathcal{D}^\circ$, $\tilde{\mathcal{D}}(v) = \tilde{g}(v)\mathcal{D}^\circ$, $\tilde{g}(v) > 1$ being a geometric factor). Introducing two characteristic free volumes, a critical free volume v^*, large enough to permit a substantial displacement, and v^f, the average free volume per molecule, they expressed the diffusion coefficient by

$$\mathcal{D} \simeq \tilde{g}(v^*)\mathcal{D}^\circ e^{-\lambda v^*/v^f}, \tag{21}$$

where λ is a numerical constant (which need not be the same for translation or rotation; cf. below). The average free volume is assumed to arise from the thermal expansion at constant pressure, which can be

approximately written as:

$$v^f = \alpha\bar{v}(T - T_0), \tag{22}$$

where α and $\bar{v}$ are mean values of the thermal expansion coefficient and the molecular volume, and T_0 is the temperature at which the volume per molecule is reduced to the close-packing limit. Let δv denote the difference between v^* and v^f, so $\delta v = v^* - v^f$. Substituting Eq. 22 into Eq. 21 one obtains the result of Cohen and Turnbull (1959):

$$\begin{aligned}\mathcal{D} &= \tilde{g}(v^*)\mathcal{D}^\circ(T)e^{-\lambda v^*/[\alpha\bar{v}(T-T_0)]} \\ &= g\mathcal{D}^\circ(T)e^{-\beta/(T-T_0)},\end{aligned} \tag{23}$$

where $g = \tilde{g}(v^*)e^{-\lambda}$ and $\beta = \lambda\delta v/\alpha\bar{v}$. Eq. 23 was developed for a simple liquid of hard spheres and was successfully applied to explain the fluidity of a large number of glass-forming substances.

Diogo and Martins (1982) have applied a similar approach to explain the temperature dependence of viscosities of thermotropic nematic liquid crystals. Because the nematic viscosities can be associated with both the translational and rotational diffusivities of the nematogen molecules, Diogo and Martins (1982) had to consider both types of molecular mobility. We now use the result of Cohen and Turnbull and estimate the critical free volume v^*, and the small-scale diffusion $\mathcal{D}^\circ(T)$, in a manner somewhat related to that of Diogo and Martins, to calculate diffusion coefficients for rotational and translational motions of molecules in liquid crystalline phases.

Let us use diffusion in the isotropic phase of the liquid crystalline material as the reference. Let us thus define the critical free volume for the isotropic phase, $v^* = v^f_{iso} + \delta v$, where v^f_{iso} is an average free volume per molecule and δv is an increase in the free volume sufficient for the displacement, and $\mathcal{D}^\circ_{iso}(T)$ is the small-scale diffusion coefficient in the isotropic phase. (Here, $\mathcal{D}$ denotes either the translational diffusion coefficient D or the rotational diffusion coefficient R.) Then the diffusion coefficient is given by Eq. 23 with $\mathcal{D}^\circ(T) \equiv \mathcal{D}^\circ_{iso}(T)$:

$$\mathcal{D}_{iso}(T) = g_{iso}\,\mathcal{D}^\circ_{iso}(T)e^{-\beta_{iso}/(T-T_0)}, \tag{24}$$

where $\beta_{iso} = \lambda \cdot \delta v/(\alpha_{iso}\bar{v}_{iso})$. We note here that the critical free volume for rotation and for translation should, in general, be different, and this is also true for the numerical factor λ. However, in a liquid of rodlike particles the large-scale rotational diffusion about the short axis, and the translational diffusion parallel to this axis are strongly coupled (see, for example, Doi and Edwards [1986], and Moscicki [1985]); therefore, critical free volumes for both motions should be of comparable order. Thus, for convenience in what follows, we shall use a common critical volume, but let their differences be incorporated into the numerical factors $\lambda_R \neq \lambda_D$.

The most pronounced and important feature of liquid crystalline phases is the existence of significant orientational order such as of the long axis of the phospholipid chains. This orientational order is due to the mean ordering potential experienced by each molecule, which is usually taken to be that calculated by Maier and Saupe or Marcelja in the mean field approximation (Martire, 1979):

$$U(\theta) = -\rho(p, T)bS\,\frac{3\cos^2\theta - 1}{2}, \tag{25}$$

where θ is the angle between the long axis of the molecule and the direction of the average orientation (the director), S is the (nematic) order parameter defined as $S = \int[(3\cos^2\theta - 1)/2] \cdot e^{-U(\theta)/\mathcal{R}T}\,d\theta$, and $\rho(p, T)$ is the number density, and b is the interaction constant. [Because it was developed originally for the nematic phase, the ordering potential is customarily referred to as the nematic potential, although it is also relevant to the ordering of liquid crystalline molecules in more complicated phases such as those of model membranes.]

The ordering of the long molecular axis produces a decrease in the average free volume at the disposal of a molecule. Therefore, if the molecule is to gain the critical free volume v^*, the cage has to expand considerably, first by an amount it was reduced by the nematic order Δv_{or}, and, additionally, by an amount δv, sufficient to reach the size of v^*, which is needed for the displacement. This can be written as $v^* = v^f_{iso} + \delta v = (v^f_{or} + \Delta v_{or}) + \delta v$, with v^f_{or} and v^f_{iso} being average free volumes per molecule in ordered and isotropic phases, respectively.

To estimate Δv_{or} we proceed as follows. Let k be the isothermal compressibility of the ordered phase and V_{or} be the volume per particle in the ordered phase. Then, by definition,

$$k = -\frac{1}{V_{or}}\left(\frac{\partial V}{\partial p}\right)_T. \tag{26}$$

If Δp_{or} denotes the associated fluctuation in the pressure leading to increase of the size of the cage by Δv_{or}, then assuming that the temperature remains constant one can write:

$$k \simeq -\frac{1}{V_{or}}\frac{\Delta v_{or}}{\Delta p_{or}}. \tag{27}$$

This should produce a change in the free energy per molecule: $\Delta G_{or} = V_{or}\Delta p_{or}$, provided the ordered phase is otherwise at equilibrium. On the one hand, this change can be written in terms of Eq. 27

$$\Delta G_{or} = V_{or}\Delta p_{or} = -\frac{1}{k}\Delta v_{or}. \tag{28}$$

On the other hand, because the temperature is constant, the change in the free energy can be associated with the change of the average energy of intermolecular anisotropic interactions, which in terms of the Maier-Saupe mean field approximation can be written as (Martire, 1979):

$$\Delta G_{or} = -\frac{1}{2}\rho(p, T)bS^2. \tag{29}$$

Thus, by comparing Eqs. 28 and 29, one obtains

$$\Delta v_{or} = [k\rho(p, T)b/2] \cdot S^2. \tag{30}$$

The critical free volume v^*, is then

$$v^* = [k\rho(p, T)b/2] \cdot S^2 + v^f_{or} + \delta v, \tag{31}$$

or, more conveniently for future use,

$$\frac{v^*}{v^f_{or}} = 1 + \frac{[k\rho(p, T)b/2] \cdot S^2 + \delta v}{v^f_{or}}. \tag{31a}$$

We note at this point that Diogo and Martins (1982) neglected $v^f_{or} + \delta v$, i.e., assumed $v^* \sim S^2$.

(One may argue whether it is appropriate to assign all the nematic energy [cf. Eq. 29] to free volume changes. Let us by contrast assume that not all the nematic energy is disposed of in the course of the free volume expansion, i.e., let $\Delta G_{or} = -\frac{1}{2}\rho(p, T)b(S^2 - S_o^2)$, where S_o is a "residual" order parameter left after the initial expansion by Δv_{or}. Then from a purely formal point of view, taking into account the residual order, Eq. 31 becomes $v^* = [k\rho(p, T)b/2] \cdot S^2 + v^f_{or} + \delta v - [k\rho(p, T)b/2] \cdot S_o^2 = [k\rho(p, T)b/2] \cdot S^2 + v^f_{or} + \delta v$, i.e., it retains its original form with respect to the S^2 dependence. Thus, we can suppress the question of the residual order without losing generality in the discussion.)

Small-scale translational or rotational diffusion can be considered to be an activation process: $\mathcal{D}^\circ(T) \sim e^{-E_D/\mathcal{R}T}$, where $\mathcal{D} = D$ or R. Because

the ordering potential essentially influences only the rotational dynamics of the long molecular axis, cases of translational diffusion and of rotational diffusion about the long axis (characterized by $R_\parallel$) are insensitive to the presence of the potential. Therefore, both diffusion processes can be written as Arrhenius-like activation processes with activation energies close to that for the isotropic phase; $\mathcal{D}^\circ \simeq \mathcal{D}^\circ_{or}(T) \simeq \mathcal{D}^\circ_{iso}(T) = D_o \exp(-E_\mathcal{D}/\mathcal{R}T)$. However, for rotational diffusion of the long axis (characterized by $R_\perp$), a molecule has to pass over an additional barrier resulting from the ordering potential. In the Maier-Saupe mean field approximately the height (the strength) of the nematic potential is $E = \rho(p, T)bS$ (cf. Eq. 25), so the net barrier should be

$$E_{R_\perp} = E_R + \rho(p, T)b \cdot S, \tag{32}$$

and the dependence of $\mathcal{D}^\circ(T) = R_\perp(T)$ upon temperature should be $\mathcal{D}^\circ(T) = R_o \exp[-(E + \rho(p, T)b \cdot S)/\mathcal{R}T]$.

Substituting the appropriate expressions for $\mathcal{D}^\circ(T)$, v^* (cf. Eq. 31a), and $v^f_{or} = \alpha_{or}\bar{v}_{or}(T - T_o)$ into Eq. 21, and rearranging as in Eq. 23, one obtains for translational diffusion and for rotational diffusion about the long axis,

$$\mathcal{D}(T, S) = g^\mathcal{D} \exp\left(-\frac{E_\mathcal{D}}{\mathcal{R}T}\right)\exp\left(-\frac{\beta_{or} + \theta S^2}{T - T_o}\right),$$
$$\mathcal{D} = D \text{ or } R_\parallel, \tag{33}$$

and for rotational diffusion about the short axis,

$$R_\perp(T, S) = g^{R_\perp}\exp\left(-\frac{E_R + \epsilon S}{\mathcal{R}T}\right)\exp\left(\frac{\beta_{or} + \theta S^2}{T - T_o}\right), \tag{34}$$

where $\epsilon = \rho(p, T)b$, $\beta_{or} = \lambda \cdot \delta v/(\alpha_{or}\bar{v}_{or})$ and $\theta = \lambda \cdot k\rho(p, T)b/2\alpha_{or}\bar{v}_{or})$.

Eqs. 33 and 34 are developed for a single component system. To apply these results to phospholipid/cholesterol mixtures we will now extend the free volume approach on the phospholipid/cholesterol binary mixture. Let subscripts "lp" and "ch" refer to properties characteristic of the phospholipid and cholesterol entity, respectively. According to the discussion of mixtures by Cotter (1977), the mean ordering potential experienced by a cholesterol molecule (probe) can be written as:

$$U_{ch}(\theta) = -\rho_o[\xi b_{ch}S_{ch} + (1 - \xi)b_{lp}S_{lp}]\frac{3\cos^2\theta - 1}{2}, \tag{35}$$

where ξ is the average number fraction of cholesterol molecules in the neighborhood of the CSL probe.

As a result, Eqs. 31–34 have to be modified. The change in the free energy becomes (cf. Eq. 31):

$$\Delta G = -\tfrac{1}{2}\rho[\xi b_{ch}S^2_{ch} + (1 - \xi)b_{lp}S_{lp}S_{ch}], \tag{36}$$

where S_{ch} is the average order parameter of cholesterol in solution. The change in the free volume due to the presence of the ordering potential is (cf. Eq. 30):

$$\Delta v_{or} = \xi\omega_{ch}S^2_{ch} + (1 + \xi)\omega_{lp}S_{lp}S_{ch} + v^f_{or} + \delta v, \tag{37}$$

where $\omega_i = k\rho_o b_i/2$ and i= "ch" or "lp". If v^f_i is the average free volume per i^{th} molecule, then v^f_{or} can be written as $v^f_{or} = \xi v^f_{ch} + (1 - \xi)v^f_{lp} = \langle\alpha\bar{v}\rangle_{ch}(T - \bar{T}_o)$, with $\langle\alpha\bar{v}\rangle_{ch} = \xi\alpha_{ch}\bar{v}_{ch} + (1 - \xi)\alpha_{lp})\bar{v}_{lp}$ and $\bar{T}_o = [\xi\alpha_{ch}\bar{v}_{ch}T_{o,chol} + (1 - \xi)\alpha_{lp}\bar{v}_{lp}T_{0,lip}]/\langle\alpha\bar{v}\rangle_{ch}$, i.e., the average free volume per cholesterol molecule can be also expressed in the form of Eq. 22.

Diffusion coefficients for translational diffusion and rotational diffusion about the long axis can be then written as:

$$\mathcal{D}(T, S_{ch}) = g^\mathcal{D}\exp\left(-\frac{E_\mathcal{D}}{\mathcal{R}T}\right)\exp\left[-\frac{\beta_{or} + \xi\theta_{ch}S^2_{ch} + (1 - \xi)\theta_{lp}S_{lp}S_{ch}}{T - \bar{T}_o}\right], \tag{38}$$

where $\mathcal{D}$ is either D or $R_\parallel$.

Because the average height of the ordering potential experienced by the cholesterol molecule is now (cf. Eq. 32):

$$E = \rho_o[\xi b_{ch}S_{ch} + (1 - \xi)b_{lp}S_{lp}], \tag{39}$$

the diffusion coefficient for the reorientation of the long axis becomes:

$$R_\perp(T, S_{ch}) = g^{R_\perp}\exp\left[-\frac{E_R + \xi\epsilon_{ch}S_{ch} + (1 - \xi)\epsilon_{lp}S_{lp}}{\mathcal{R}T}\right] \times \exp\left[-\frac{\beta_{or} + \xi\theta_{ch}S^2_{ch} + (1 - \xi)\theta_{lp}S_{lp}S_{ch}}{T - \bar{T}_0}\right], \tag{40}$$

where $\epsilon_i = \rho_o(p, T)b_i$, $\beta_{or} = \lambda \cdot \delta v/\langle\alpha\bar{v}\rangle_{ch}$ and $\theta_i = \lambda \cdot k_i\rho_o(p, T)b_i/(2\langle\alpha\bar{v}\rangle_{ch})$, and i = "ch" or "lp". Note at this point that similar expressions for diffusion coefficients of phospholipid molecules in model membranes can be derived in the same fashion.

Let us now consider Eqs. 38 and 40 in the limits which are appropriate for our experimental conditions. The first relevant limit is that of the pure phospholipid membrane, with the CSL spin label as a marker. This corresponds to $\xi \to 0$, in which case Eqs. 38 and 40 become, respectively,

$$\mathcal{D}(T, S_{ch}) = g^\mathcal{D}_{lp}\exp\left(-\frac{E_\mathcal{D}}{\mathcal{R}T}\right)\exp\left(-\frac{\beta_{lp} + \theta_{lp}S_{lp}S_{ch}}{T - T_{lp}}\right), \tag{41}$$

and

$$R_\perp(T, S_{ch}) = g^{R_\perp}_{lp}\exp\left(\frac{E_R + \epsilon_{lp}S_{lp}}{\mathcal{R}T}\right)\exp\left(\frac{-\beta_{lp} + \theta_{lp}S_{lp}S_{ch}}{T - T_{lp}}\right), \tag{42}$$

where $\epsilon_{lp} = \rho_o(p, T)b_{lp}$, $\theta_{lp} = \lambda_{lp} \cdot k_{lp}\epsilon_{lp}/(2\alpha_{lp}\bar{v}_{lp})$, and $\beta_{lp} = \lambda_{lp}\delta v/(\alpha_{lp}\bar{v}_{lp})$. T_{lp} corresponds to the temperature at which the average free volume per cholesterol molecule in the phospholipid environment is reduced to its close-packing limit. In this limit the cholesterol probe should show the orientational order similar to that of the phospholipid environment, although slightly enhanced by the rigidity and elongation of the probe, i.e., $S_{ch} > S_{lp}$.

However, when the concentration of cholesterol is significant, cholesterol molecules experience mostly the cholesterol environment ($\xi \to 1$) according to our results. (Note that $\gamma_{chol} \ll 1$.) Thus, diffusion coefficients are given by (the second limit):

$$\mathcal{D}(T, S_{ch}) = g^\mathcal{D}_{ch}\exp\left(-\frac{E_\mathcal{D}}{\mathcal{R}T}\right)\exp\left(-\frac{\beta_{ch} + \theta_{ch}S^2_{ch}}{T - T_{ch}}\right), \tag{43}$$

and

$$R_\perp(T, S_{ch}) = g^{R_\perp}_{ch}\exp\left(-\frac{E_R + \epsilon_{ch}S_{ch}}{\mathcal{R}T}\right)\exp\left(-\frac{\beta_{ch} + \theta_{ch}S^2_{ch}}{T - T_{ch}}\right), \tag{44}$$

where $\epsilon_{ch} = \rho_o(p, T)b_{ch}$, $\theta_{ch} = \lambda_{ch} \cdot k_{ch}\epsilon_{ch}/(2\alpha_{ch}\bar{v}_{ch})$, and $\beta_{ch} = \lambda_{ch}\delta v/(\alpha_{ch}\bar{v}_{ch})$. T_{ch} is the temperature at which the average free volume per cholesterol molecule in the cholesterol environment is reduced to its close-packing limit.

We have observed a saturation of S_{CSL} around $x_{chol} \sim 0.1$ for phosphatidycholine/cholesterol mixtures. This suggests that the clustering of cholesterol is appreciable when x_{chol} is as low as 0.1. This implies that ξ approaches 1 at such low mole fraction. Moreover, comparing Eqs. 38 and 40 with our experimental results (cf. Eqs. 13 and 14, and figs. 7 and 8), we concluded that $\theta_{ch} \gg \theta_{lp}$. This is in qualitative agreement with the fact that, considering the elongation and structural rigidity of the cholesterol molecule, one would expect λ_{ch} (which is the intermolecular interaction factor between cholesterol molecules) to be significantly larger than λ_{lp} (interaction factor between the cholesterol probe and the phospholipid neighborhood). We note also that because the experimental data can be fitted with Eqs. 13 and 14, which contain solely the S^2 term, β_{ch} and β_{lp} must be small also. Furthermore, our results (cf. Eqs. 13 and 14) suggest that $T_{ch} \ll T$ (cf. Eqs. 43 and 44). (That is, we can expand the denominator of the exponent in Eqs. 43 and 44 such that $1/(T - T_{ch}) \simeq 1/T(1 + T_{ch}/T)$ with $T_{ch} \ll T$, so that within experimental error $1/(T - T_{ch})$ is well approximated by $1/T$.)

Consequently, the S^2_{ch} term in Eqs. 38 and 40 becomes dominant even at very low cholesterol mole fraction. This results in the data being fitted with Eqs. 13 and 14 with the same parameters as for $x_{chol} \sim 0$ (cf. Figs. 7 and 8). Finally, our observations are consistent with a θ_{ch} for D_{CSL} being than that for $R_{\perp CSL}$. This can be reconciled with the above theory if the λ_{ch} values differ accordingly for the two types of motion, the possibility of which was noted above. Then it follows from Eq. 21 that there is a more crucial dependence on the free volume for the rational diffusion. The different temperature dependences of the S^2_{ch} terms in Eqs. 13 and 14 (i.e., $\alpha[T]$ and A, respectively) remains to be explained.

This work was supported by National Institutes of Health grant GM25862 and National Science Foundation grant DMR89-01718. Computations were performed at the Cornell National Supercomputer Facility. Dr. Moscicki acknowledges partial support of his visit to Cornell University by Polish Academy of Sciences under Project CPBP 01.12.

Received for publication 11 September 1989 and in final form 13 November 1989.

REFERENCES

Alecio, M. R., D. E. Golan, W. R. Veatch, and R. R. Rando. 1982. Use of fluorescent cholesterol derivative to measure lateral mobility of cholesterol in membranes. *Proc. Natl. Acad. Sci. USA.* 79:5171–5174.

Cleary, D. A., Y.-K. Shin, and J. H. Freed. 1988. Rapid determination of translational diffusion coefficients using ESR imaging. *J. Magn. Res.*79:474–492.

Cohen, M. H., and D. Turnbull. 1959. Molecular transport in liquids and glasses. *J. Chem. Phys.* 31:1164–1169.

Cotter, M. A. 1977. Consistency of mean field theories of nematic liquid crystals. *Mol. Cryst. Liq. Cryst.* 39:173–181.

Crepeau, R., S. Rananavare, and J. H. Freed. 1987. Automated least squares fitting of slow motional ESR spectra. Abstracts of the 10th International EPR Symposium. Rocky Mountain Conference. Denver, CO.

de Gennes, P. G. 1974. The Physics of Liquid Crystals. Oxford University Press, London. 23

De Kruyff, B., P. W. M. Van Vijck, R. A. Demel, A. Schuijff, F. Brants, and L. L. M. Van Deenen. 1974. Non-random distribution of cholesterol in phosphatidylcholine bilayers. *Biochim. Biophys. Acta.* 356: 1–7.

Diogo, A. C., and A. F. Martins. 1982. Order parameter and temperature dependence of the dynamic viscosity of nematic liquid crystals *J. Physique.* 43:779–786.

Doi, M., and S. F. Edwards. 1986. Theory of Polymer Dynamics. Clarendon Press, Oxford, UK. 324–336.

Freed, J. H. 1976. The theory of slow tumbling ESR spectra for nitroxides. *In* Spin Labeling, Theory and Applications. L. J. Berliner, editor. Academic Press, Inc., New York. 53–132.

Hornak, J. P., J. K. Moscicki, D. J. Schneider, and J. H. Freed. 1986. Diffusion coefficients in anisotropic fluids by ESR imaging of concentration profiles. *J. Chem. Phys.* 84:3387–3395.

Jost, P. C., and O. H. Griffith. 1973. The molecular reorganization of lipid bilayers by osmium tetraoxide. A spin-label study of orientation and restricted *y*-axis anisotropic motion in model membrane system. *Arch. Biochem. Biophys.* 159:70–81.

Kar, L., E. Ney-Igner, and J. H. Freed. 1985. Electron spin resonance and electron-spin-echo study of oriented multilayers of L_α-phosphatidylcholine water systems. *Biophys. J.*48:569–593.

Korstanje, L. J., E. E. van Faassen, and Y. K. Levine. 1989. Slow motion ESR study of order and dynamics in oriented lipid multilayers: effect of unsaturation and hydration. *Biochim. Biophys. Acta.* 980:225–233.

Kusumi, A., W. K. Subczynski, M. Pasenkiewicz-Gierula, J. S. Hyde, and H. Merkle. 1986. Spin-label studies on phosphatidylcholine-cholesterol membranes: effect of alkyl chain length and unsaturation in the fluid phase. *Biochim. Biophys. Acta.* 854:307–317.

Lindblom, G., L. B. A. Johansson, and G. Arvidson. 1981. Effect of cholesterol in membranes. Pulsed nuclear magnetic resonance measurement of lipid lateral diffusion. *Biochemistry.* 20:2204–2207.

Martire, D. E. 1979. Theory of binary mixtures. *In* The Molecular Physics of Liquid Crystals. G. R. Luckhust and G. W. Gray, editor. Academic Press, Inc., London. 239–261.

Meirovitch, E., and J. H. Freed. 1984. Molecular configuration, intermolecular interactions and dynamics in smectic liquid crystals from slow motional ESR lineshapes. *J. Phys. Chem.* 88:4995–5004.

Meirovitch, E., D. Igner, E. Igner, G. Moro, and J. H. Freed. 1982. Electron spin relaxation and ordering in smectic and supercooled nematic liquid crystals. *J. Chem. Phys.* 77:3915–3938.

Merkle, H., W. Subczynski, and A. Kusumi. 1987. Dynamic fluorescence quenching studies on lipid mobilities in phosphatidylcholine-cholesterol membranes. *Biochim. Biophys. Acta.* 897:238–248.

Moscicki, J. K. 1985. Molecular dynamics in rigid-rod macromolecular lyotropic liquid crystals. *Adv. Chem. Phys.* 63:631–714.

Moscicki, J., Y.-K. Shin, and J. H. Freed. 1989. Dynamic imaging of diffusion by ESR. *J. Magn. Res.* 84:554–572.

Moscicki, J. K., Y.-K. Shin, and J. H. Freed. 1990. The method of dynamic imaging of diffusion by ESR. *In* EPR Imaging and In Vivo EPR. G. Eaton, S. Eaton, and K. Ohno, editors. CRC Press, Inc., Boca Raton, FL. In press.

Presti, F. T., and S. I. Chan. 1982. Cholesterol-phospholipid interaction in membranes. I. Cholestane spin label studies of phase behavior of cholesterol-phospholipid liposomes. *Biochemistry.* 21:3821–3830.

Recktenwald, D. J., and H. M. McConnell. 1981. Phase equilibria in binary mixtures of phosphatidylcholine and cholesterol. *Biochemistry.*20:4505–4510.

Rubenstein, J. L. R., B. A. Smith, and H. M. McConnell. 1979. Lateral diffusion in binary mixtures of cholesterol and phosphatidylcholines. *Proc. Natl. Acad. Sci. USA.* 76:15–18.

Schneider, D. J., and J. H. Freed. 1989. Calculating slow motional magnetic resonance spectra: a user's guide. *In* Biological Magnetic Resonance. Vol. 8. L. J. Berliner and J. Reuben, editors. Plenum Publishing Corp., New York. 1–76.

Shimshik, E. J., and H. M. McConnell. 1973. Lateral phase separation in phcsphclipid membranes. *Biochemistry*. 12:2351–2360.

Shin, Y.-K., and J. H. Freed. 1989*a*. Dynamic imaging of lateral diffusion by electron spin resonance and study of rotational dynamics in model membranes. Effect of cholesterol. *Biophys. J.* 55:537–550.

Shin, Y.-K., and J. H. Freed. 1989*b*. Thermodynamics of phosphatidylcholine-cholesterol mixed model membranes in the liquid crystalline state studied by the orientational order parameter. *Biophys. J.* 56:1093–1100.

Tanaka, H., and J. H. Freed. 1984. Electron spin resonance studies on ordering and rotational diffusion in oriented phosphatidylcholine multilayers: evidence for a new chain ordering transition. *J. Phys. Chem.* 88:6633–6644.

Van Dijck, P. W. M., B. De Kruijff, L. M. Van Deenen, J. De Gier, and R. A. Demel. 1976. The preference of cholesterol for phosphatidylcholine in mixed phosphatidylcholine-phosphatidylethanolamine bilayers. *Biochim. Biophys. Acta.* 455:576–587.

Vaz, W. L. C., R. M. Clegg, and D. Hallmann. 1985. Translational diffusion of lipids in liquid crystalline phase phosphatidylcholine multilayers. A comparison of experiment with theory. *Biochemistry*. 24:781–786.

Verkleij, A. J., P. H. J. Th. Ververgaert, B. de Kruyff, and L. L. M. Deenen. 1974. The distribution of cholesterol in bilayers of phosphatidylcholines as visualized by freeze fracturing. *Biochim. Biophys. Acta.*373:495–501.